The prion protein is critical for DNA repair and cell survival after genotoxic stress

Anne Bravard, Frédéric Auvré, Damiano Fantini, Jacqueline Bernardino-Sgherri, Ludmilla Sissoëff, Mathieu Daynac, Zhou Xu, Olivier Etienne, Capucine Dehen, Emmanuel E Comoy, et al.

904–916 *Nucleic Acids Research, 2015, Vol. 43, No. 2* *Published online 24 December 2014*
doi: 10.1093/nar/gku1342

The prion protein is critical for DNA repair and cell survival after genotoxic stress

Anne Bravard[1,2,3,4], Frédéric Auvré[1,2,3,4], Damiano Fantini[1,2,3,4], Jacqueline Bernardino-Sgherri[1,2,3,4], Ludmilla Sissoëff[5], Mathieu Daynac[1,2,3,4], Zhou Xu[5], Olivier Etienne[1,2,3,4], Capucine Dehen[5], Emmanuel Comoy[5], François D. Boussin[1,2,3,4], Gianluca Tell[6], Jean-Philippe Deslys[5] and J. Pablo Radicella[1,2,3,4,*]

[1]CEA, Institute of Cellular and Molecular Radiobiology, F-92265 Fontenay-aux-Roses, France, [2]INSERM, U967, F-92265 Fontenay-aux-Roses, France, [3]Université Paris Diderot, UMR 967, F-92265 Fontenay-aux-Roses, France, [4]Université Paris Sud, UMR 967, F-92265 Fontenay-aux-Roses, France, [5]CEA, Institut des Maladies Emergentes et des Thérapies Innovantes, Service d'Etudes des Prions et des Infections Atypiques, F-92265 Fontenay-aux-roses, France and [6]Department of Medical and Biological Sciences, University of Udine, I-33100 Udine, Italy

Received July 16, 2014; Revised December 11, 2014; Accepted December 13, 2014

ABSTRACT

The prion protein (PrP) is highly conserved and ubiquitously expressed, suggesting that it plays an important physiological function. However, despite decades of investigation, this role remains elusive. Here, by using animal and cellular models, we unveil a key role of PrP in the DNA damage response. Exposure of neurons to a genotoxic stress activates *PRNP* transcription leading to an increased amount of PrP in the nucleus where it interacts with APE1, the major mammalian endonuclease essential for base excision repair, and stimulates its activity. Preventing the induction of *PRNP* results in accumulation of abasic sites in DNA and impairs cell survival after genotoxic treatment. Brains from *Prnp*$^{-/-}$ mice display a reduced APE1 activity and a defect in the repair of induced DNA damage *in vivo*. Thus, PrP is required to maintain genomic stability in response to genotoxic stresses.

INTRODUCTION

PrP^{Scr}, a conformational isoform of the prion protein PrP, is well known for its role as an infectious agent in a series of fatal neurodegenerative diseases characterized by extensive brain spongiform degeneration, widespread neuronal loss, synaptic alteration and atypical brain inflammation. However, the physiological role of PrP remains elusive. Its high degree of conservation suggests that it has an important function (1–3). The demonstration that transgenic mice expressing PrP proteins deleted of specific domains exhibited major neurodegeneration (4,5) supports this view. Its neuroprotective effect against oxidative stress has been repeatedly demonstrated in cell studies (6–8) and, interestingly, the only obvious phenotype of PrP-null mice is their higher sensitivity to conditions known to generate oxidative stress including hypoxia (9) and ischemia (10). Several, non-exclusive, hypotheses to explain this protective effect have been proposed: antioxidant activity, metal homeostasis and apoptosis regulation (1,11). However, although DNA is a major target for reactive oxygen species induced toxicity and expression of PrP was shown to protect human neuronal cells against DNA damage, both under basal conditions and following exposure to oxidative stress (12,13), one possibility that to our knowledge has never been explored is that PrP could have a direct role in DNA repair. Oxidative DNA damage is the most frequent type of lesion formed in DNA and it includes modified bases, apurinic/apyrimidinic (AP) sites and single strand breaks, all of them substrates of the base excision repair (BER) pathway (14). A major player in this pathway is the AP endonuclease APE1. Knockout of *Ape1* in mice causes embryonic lethality (15,16) and *APE1*-knockdown in cells triggers cell death (17). Studies on mice heterozygous for the *Ape1* gene show that the level of APE1 is critical for the cell response to genotoxic stresses (16,18). In particular, APE1 DNA repair activity is crucial for the survival of neuronal cells subjected to oxidative stress (19–21).

Thus, to address the question of a role for PrP in DNA damage repair in neuronal cells, we explored whether changes in PrP levels could have an effect on the regulation of BER either on unstressed cells or in cells exposed to a genotoxic challenge by methyl-methane sulfonate (MMS), a compound that reacts with DNA directly avoiding the pleiotropic effects of an oxidative stress. We show here that

*To whom correspondence should be addressed. Tel: +33 1 46 54 88 57; Fax: +33 1 46 54 91 38; Email: pablo.radicella@cea.fr
Correspondence may also be addressed to Anne Bravard. Tel: +33 1 46 54 89 53; Fax: +33 1 46 54 91 38; Email: anne.bravard@cea.fr

PrP expression is induced and the protein stimulates APE1 enzymatic activity in the nucleus of cells exposed to genotoxic insult, thereby conferring resistance to the stress.

MATERIALS AND METHODS

Animals

Mice were bred and maintained according to the guidelines for the care and use of laboratory animals of the French Ministry of Agriculture. The *Prnp*$^{-/-}$ mice (22,23), which had a genetic background derived from 129/Sv and C57BL/6J, have been back-crossed for 13 generations and then cross-bred to obtain a pure C57BL/6N genetic background. Wild-type C57BL/6N mice (*Prnp*$^{+/+}$) were obtained from Harlan. The effect of MMS was studied on brains of 10-week-old animals sacrificed 24 h after intraperitoneal injection of vehicle dimethyl sulfoxide (DMSO) or MMS. Brains were collected and cut in half along the midsagittal plane. From one half 20% (w/v) homogenates were prepared for biochemical studies in 5% sterile glucose by using a RiboLyser (Bio-Rad). The other half was fixed by immersion overnight at 4°C in 10% neutral buffered formalin and processed for paraffin embedding using a Tissue-tek VIP processor (Leica). Five micrometer coronal (hippocampus) sections were then obtained with a microtome (RM 2125 RT, Leica) and mounted onto glass slides. Sections from, *Prnp*$^{-/-}$, *Prnp*$^{+/+}$ control and treated with MMS were mounted on the same slide and used for confocal and immunohistological analysis.

Cell culture and genotoxic treatments

The immortalized murine hippocampal *Prnp*$^{-/-}$ cell line HpL3–4 (22) was stably transfected via retroviral expression vectors expressing or not mouse *Prnp*. Cells were grown in OptiMEM-Glutamax (Gibco) supplemented with 10% fetal calf serum (FCS) and antibiotics. The human neuroblastoma SH-SY5Y cell line was grown in DMEM-Glutamax (Gibco) with 10% FCS and antibiotics. Primary cultures of neural stem and progenitor cells were prepared from freshly dissociated subventricular zone of 'wild-type' or *Prnp*$^{-/-}$ mouse brains. Cells were plated in laminin-coated (Sigma) 12-well plates and cultured in Neurocult complete medium (StemCell) supplemented with heparin (2 μg/ml), epidermal growth factor (EGF) (20 ng/ml; Invitrogen) and FGF2 (10 ng/ml; Invitrogen) as previously described (24). For MMS treatments, cells were incubated for 1 h at 37°C in complete medium with various concentration of MMS. Cells were then washed and returned to the incubator in fresh medium for the indicated recovery periods. When indicated, actinomycin D was added at a final concentration of 5 μg/ml 1 h before MMS treatment and maintained thereafter during the treatment and the recovery period. Oxidative stress was induced by incubating cells for 24 h in medium containing hydrogen peroxide at the indicated concentrations.

Cell viability was measured by cell counting using the Countess automatic cell counter (Invitrogen) after trypan blue staining and by the neutral red methods. Cells were incubated for 1 h at 37°C in medium containing 0.07% (w/v) of red neutral dissolved in cell culture medium, washed twice with Dulbecco's Phsophate-Buffered Saline (DPBS). Cell lysis was then performed by adding 1% acetic acid, 50% ethanol solution and the optical density was measured at 540 nm.

Plasmids and expression of recombinant proteins

Full-length recombinant PrP (ovine and human), ovine N-terminal mutant (PrP23-124) and N-terminus deletion (PrP103-232) mutant were produced and purified as described (25). None of the purified PrP preparations presented an intrinsic AP endonuclease activity (Supplementary Figure S5A). The constructs pGex3X-hAPE1, pGex3X-NΔ33hAPE1 and pGex3X-hAPE1K5 mutant (K24A, K25A, K27A, K31A, K32A) and their purification were described elsewhere (26). XRCC1-purified recombinant human protein was obtained as previously described (27).

Transfections

Transfections of SH-SY5Y with empty pcDNA3 or pcDNA3 MoPrP were done 24 h before treatment of cells with MMS following a standard Lipofectamine 2000 protocol (Invitrogen). siRNA corresponding to the human *PRNP* gene was synthesized by Eurogentec. The specific human siRNA sequence used was: 5′-GCC-GAG-UAA-GCC-AAA-AAC-CTT-3′ (sense). A scramble siRNA sequence (5′-CCG-AGA-AGU-AAA-GCC-AAC-CTT-3′) was used as control. Cells were grown for 24 h before being transfected with the siRNA sequences using the siRNAmax reagent (Invitrogen). They were allowed to grow for 48 h before genotoxic treatments.

Western blot analysis

The 20 000 x g cell extracts were obtained by sonication of cell pellets or brain homogenates in 20-mM Tris-HCl, pH 7.5, 250-mM NaCl, 1-mM ethylenediaminetetraacetic acid containing a cocktail of protease inhibitors: apoprotein, antipain and leupeptin (0.8 μg each). The homogenate was centrifuged at 20 000 x g for 30 min and aliquots of the supernatant were stored at −80°C for biochemical assays. Fifty microgram of total proteins from cells extracts and 5 μg of total proteins from brain extracts were loaded and resolved by sodium dodecyl sulphate-polyacrylamide gel electrophoresis (SDS-PAGE) and probed for detection of PrP with primary monoclonal antibodies SAF70 for cells extracts or SAF83 for brain extracts (Jacques Grassi, CEA Saclay). APE1 detection was done as described (28). ß actin (1/1000 Sigma) or vinculin (1/4000 Abcam) detection was used as a control for protein loading. Secondary antibodies coupled with horseradish peroxidase (Amersham) were used at 1/30 000. Detection was performed using ECL-advance Kit (Amersham).

AP endonuclease activity

AP endonuclease activity was measured using a 34-mer oligonucleotide containing a single tetrahydrofuranyl residue at position 16 and labeled as described (26). The

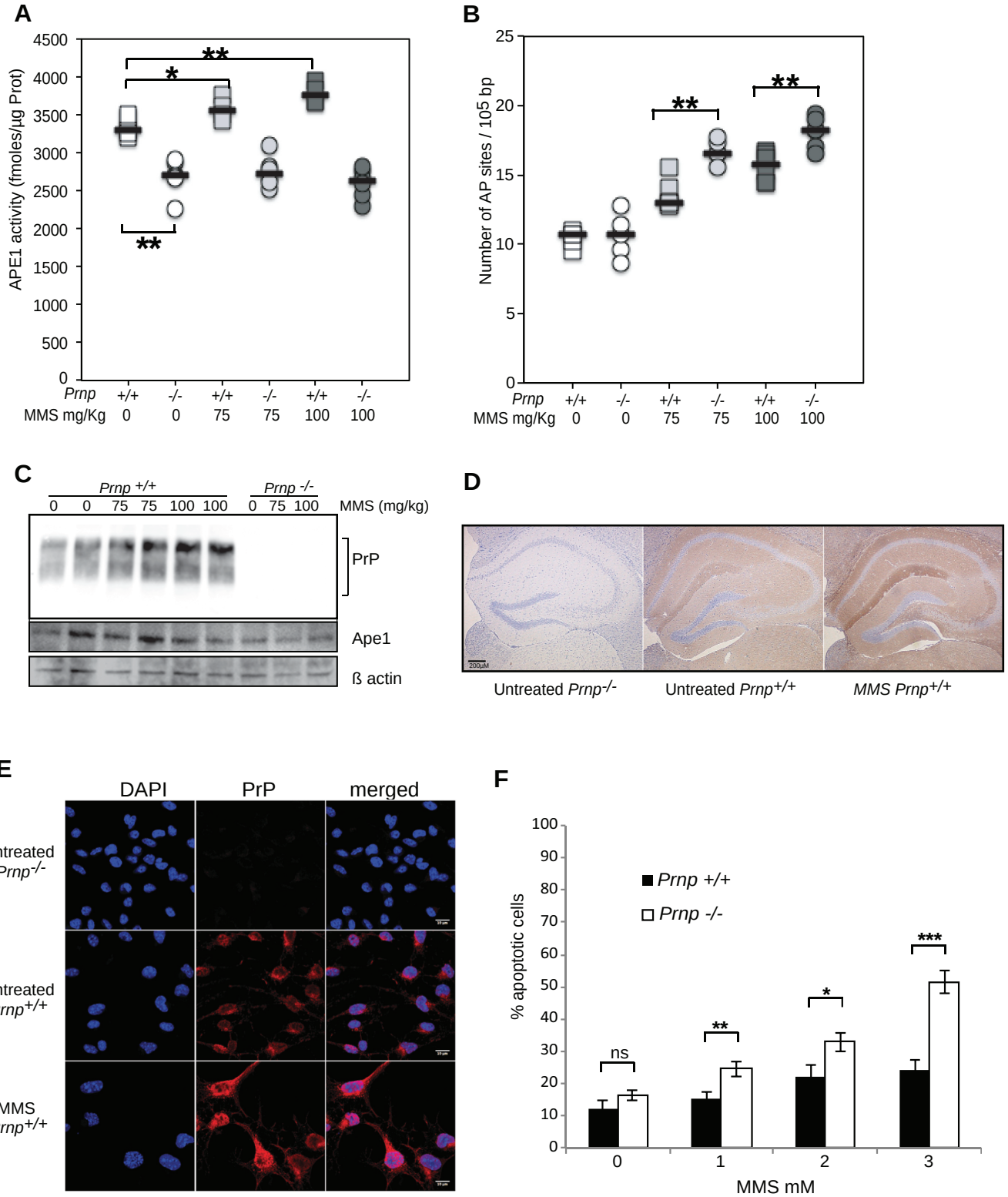

Figure 1. DNA repair is impaired in the brain from $Prnp^{-/-}$ mice. (**A–D**) Results obtained on brain samples 24 h after *in vivo* MMS treatment of $Prnp^{+/+}$ and $Prnp^{-/-}$ mice as compared to untreated mice. (A) APE1 endonuclease activity and (B) number of AP sites. Individual values as well as the median (bold line) are shown. (*$P < 0.05$; **$P < 0.01$). (C) Western blot showing the levels of PrP and APE1 proteins after MMS treatment. ßactin was used as loading control. (D) Increase in PrP immunohistochemical staining of the hippocampus of $Prnp^{+/+}$ animals treated with MMS (100 mg/kg). (**E**) PrP expression is induced in primary cultures of neural stem and progenitor cells 24 h after 1 h of treatment with 2-mM MMS. Equivalent cultures obtained from $Prnp^{-/-}$ animals were used as a negative control. (**F**) Increased apoptosis as measured by TUNEL assay on neural and progenitor cells from $Prnp^{-/-}$ animals 6 h after 1-h exposure to MMS at the indicated concentrations. One thousand cells were analyzed for each point: *$P < 0.05$; **$P < 0.01$; ***$P < 0.001$.

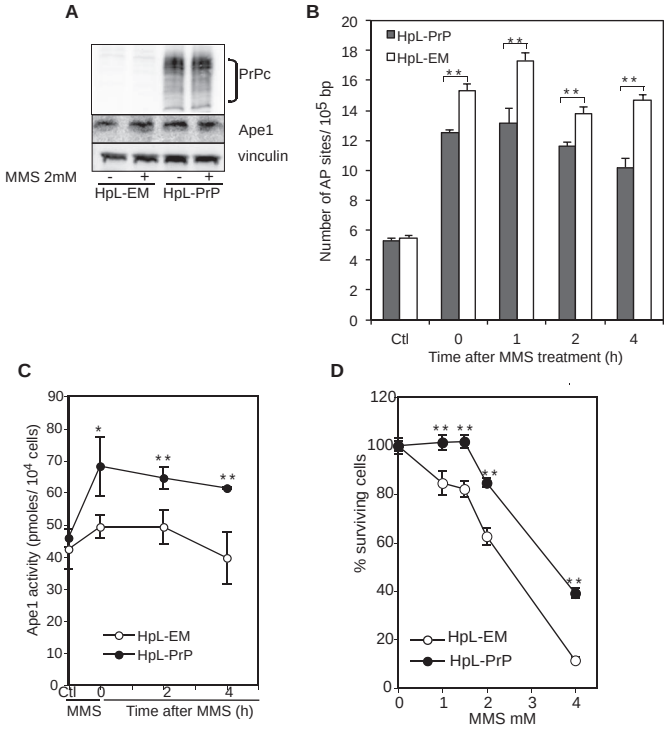

Figure 2. PrP expression in hippocampal cells from $Prnp^{-/-}$ mouse improves DNA repair and cell survival after genotoxic stress. (**A**) Western blot showing the levels of PrP and APE1 proteins in HpL3–4 cells stably expressing PrP (HpL-PrP) compared to cells carrying the empty vector (HpL-EM), 24 h after 1-h exposure with 2-mM MMS. Vinculin was used as loading control. (**B**) Number of AP sites in untreated (Ctl) and at 0, 1, 2 and 4 h following treatment with 2-mM MMS in HpL-EM and HpL-PrP cells. Mean ± SD ($n = 3$). (**C**) APE1 endonuclease activity in untreated (Ctl) and at 0, 2 and 4 h following treatment with 2-mM MMS in HpL-EM and HpL-PrP cells. Mean ± SD ($n = 3$). (**D**) Cell survival as determined by the red neutral assay for HpL-PrP cells compared to HpL-EM cells, 24 h after 1-h exposure with MMS. Mean ± SD ($n = 8$); $*P < 0.05$; $**P < 0.01$.

same protocol was used to study the *in vitro* APE1 stimulation, except that recombinant proteins and the fluorescent tetrahydrofuran-containing oligonucleotide were incubated for 15 min on ice before starting the reaction.

Quantification of DNA damage

Genomic DNA from MMS-treated or untreated cells was prepared using the QiAmp^R DNA Kit (Qiagen). AP sites were then measured using the DNA Damage Quantification kit (AP sites) from Dojindo Molecular Technologies according to the manufacturer's specifications. To validate the test, the levels of AP sites were determined in cells exposed to increasing concentrations of MMS (Supplementary Figure S1A, left panel). To rule out a significant effect of the 10-min heating step in generating additional AP sites by depurination of the alkylated bases, we compared the yield of AP sites in DNA from MMS-treated cells obtained by DNAzol (Life Technologies) including or not a 10-min heating step at 56°C (Supplementary Figure S1A, right panel). No significant differences were observed in the levels of AP sites determined using the various protocols

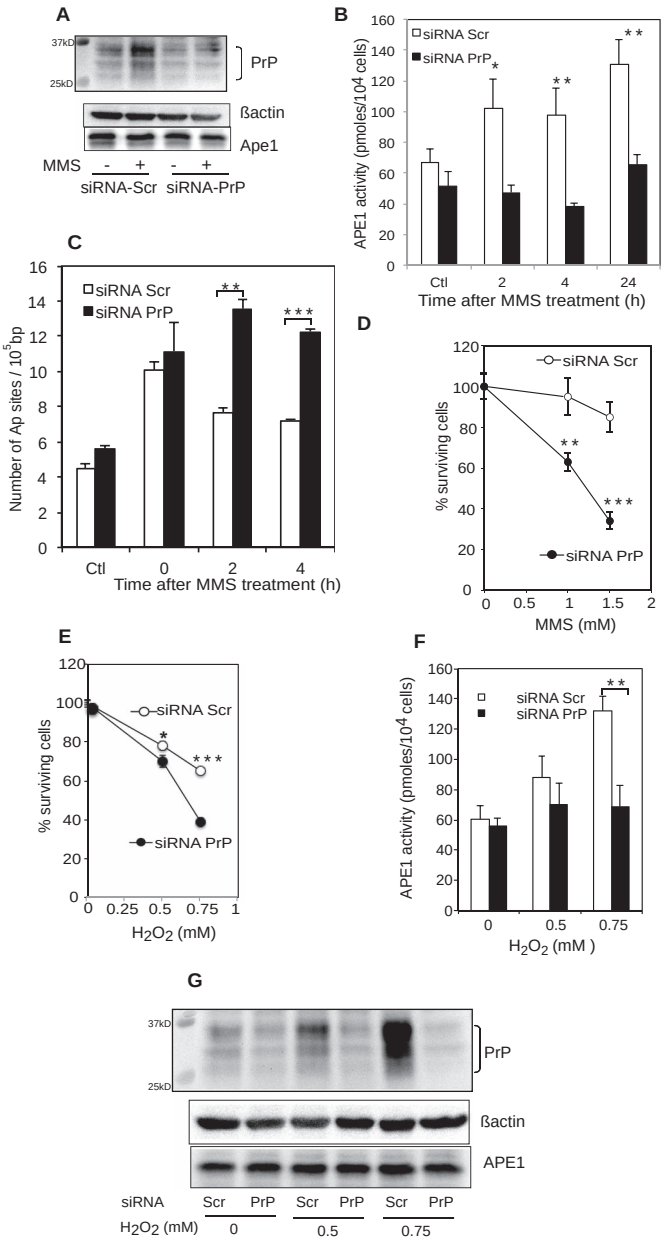

Figure 3. Downregulation of *PRNP* leads to blockage of DNA repair and decreased survival of neuronal cells after genotoxic stress. (**A**) PrP levels are induced after MMS treatment. Western blot for PrP and APE1 proteins in cell extracts from SH-SY5Y cells transfected with siRNA PrP or with the scramble siRNA after 24 h recovery in fresh medium following 1-h treatment with 1.5-mM MMS. ßactin was used as loading control. AP endonuclease activity (**B**) and AP sites (**C**) in SH-SY5Y expressing the indicated siRNAs and treated or not (Ctl) with 1.5-mM MMS. Mean ± SD ($n = 3$); $**P < 0.01$. $***P < 0.001$. (**D**) PrP-depletion sensitizes cells to MMS. SH-SY5Y cells transfected with a siRNA PrP or a scramble siRNA were treated for 1 h with MMS and cell survival was measured after 24 h of recovery. Mean ± SD ($n = 8$); $**P < 0.01$; $***P < 0.001$. (**E**) PrP-depletion sensitizes cells to H_2O_2. SH-SY5Y cells transfected with siRNA PrP or a scramble siRNA were treated with H_2O_2 and cell survival was measured 24 h later. Mean ± SD ($n = 5$); $*P < 0.05$; $***P < 0.001$. (**F**) APE1 endonuclease activity in extracts from SH-SY5Y cells 24 h after treatment with 0.5- or 0.75-mM H_2O_2. Mean ± SD ($n = 3$); $**P < 0.01$. (**G**) Western blots for PrP and APE1 proteins in cell extracts from SH-SY5Y cells transfected with siRNA PrP or a scramble siRNA after 24 h of treatment with H_2O_2. ßactin was used as loading control.

with or without a heating step for the MMS concentrations ≤2 mM used for the rest of the experiments.

Reverse transcription and QPCR

Total RNA was prepared from frozen cell pellets using RNeasy^{R} Plus kit (QIAGEN) and quantified by Nanodrop spectrophotometer. For the first strand cDNA synthesis 500 ng of total RNA was reverse-transcribed using SuperScriptVILO cDNA synthesis kit (Invitrogen, Cergy Pontoise, France). Quantitative PCRs were performed with an ABI PRISM 7300 sequence detection system (Applied Biosystems) by using the TaqMan Universal PCR Master Mix (Applied Biosystems). Quantification of each gene expression was calibrated using a reference standard curve obtained by serial dilutions of PCR product prepared from a control cDNA. The mean expression of *rplpo* (large ribosomal protein gene) was used to normalize the expression of *PRNP* gene. *PRNP* was amplified by PCR primers purchased from Applied Biosystems (Hs01920617-s1).

Immunofluorescence and confocal microscopy

For cellular analysis, cell cultures were grown on 12-mm coverslips. After the treatments they were fixed with 4% formaldehyde and, unless indicated, permeabilized in phosphate buffer saline (PBS), 0.1% Triton X-100 for 2 min at room temperature. After 10 min of blockage in PBS, 1% bovine serum albumin (BSA), they were incubated with mouse anti-PrP (SAF37 recognizing epitopes 79–92 or SAF70 recognizing epitopes 142–160), rabbit anti-APE1 (28) or rabbit anti-Histone H4 Lys12 (Santa Cruz). Alexa 594-coupled and Alexa 488-coupled secondary antibodies (Life technologies A11005 and A11008) were then used.

Coronal sections (5 μm) of adult brain hippocampus were mounted onto glass slides and treated successively with xylene, ethanol in decreasing concentrations and water. Slides were then microwaved (620 W) twice for 10 min in 10-mM citrate buffer. After washing with water the slides were treated for 1 h at room temperature with a solution containing 10% sodium lauroyl sarcosinate, 10% Triton and 2-M urea. After 1-h blockage in PBS containing 15% fetal bovine serum, the tissue was stained with a rabbit monoclonal antibody against PrP (Epitomics, clone EP 1802Y) and Alexa 488-coupled secondary antibodies (Molecular Probes).

Coverslips were mounted in Vectashield hard set^{TM} mounting medium containing 4′,6-diamidino-2-phenylindole (DAPI) (Vector). Image acquisition was performed with a Leica TCS SPE confocal microscope. Images were processed and analyzed using Image J software.

TUNEL assay

For TUNEL studies primary neuronal cells obtained from *Prnp*$^{+/+}$ and *Prnp*$^{-/-}$ animals grown on Lab-Tek (Dutscher) were treated for 1 h with 1, 2 or 3-mM MMS, washed with culture medium and returned for 6 h in the incubator at 37°C. They were then fixed for 10 min in 4% paraformaldehyde and permeabilized in PBS containing 0.1% Triton X-100 for 10 min. After a wash in PBS, cells were incubated in the dark for 1 h at 37°C, with the enzyme and the label solution provided by the '*In Situ* Cell Death Detection Kit, Fluorescein' (Roche Diagnostic). Nuclear staining was achieved by incubation with DAPI. Slides were mounted under Fluoromount (Southern Biotechnologies Associates). Apoptosis was measured by counting TUNEL positive cells visualized by fluorescence microscopy. For each point a minimum of 1000 cells were analyzed.

Proximity ligation assays

To detect protein–protein interactions, *in situ* proximity ligation assays (PLAs) (29) were performed using Duolink II secondary antibodies and detection kit (Olink Bioscience) according to the manufacturer's instructions. The specificity of this assay was assessed by using the secondary antibodies alone. No signal was detected (data not shown). The specificity of the staining was also confirmed by the lack of staining of PrP/APE1 in unstressed SH-SY5Y cells, (see Figure 6A, upper panels) and by the absence of staining of PrP/XRCC1 in MMS-treated cells (Supplementary Figure S4) (XRCC1 antibody was from Abcam). Images were acquired on a Leica TCS SPE confocal microscope and analyzed using Image J software.

Glutathion S-Transferase (GST) pull-down assay

Beads were first saturated with bait proteins by incubating 1 nmol of GST-APE1 or GST alone on 10 μl of glutathione-Sepharose 4B beads (GE Healthcare). Beads were washed four times in PBS, then 150 μg of a protein extract from MMS-treated SH-SY5Y cells was added and incubated for 2h at 4°C under gentle rocking. Beads were washed four times with PBS and then boiled in 1× Laemmli sample buffer containing 100-mM Dithiothreitol (DTT). Samples were separated on SDS-PAGE gels before western blotting.

Immunoprecipitation

5.10^6 MMS-treated or untreated SH-SY5Y cells were resuspended in 500 μl buffer A (150-mM Tris-HCl, pH 7.5, 150-mM NaCl, 0.5% Triton X-100, 1-mM $MgCl_2$ and protease inhibitors) and incubated for 15 min at 4°C on a rotating shaker. After 20-min centrifugation at 15 000 x g at 4°C, the supernatant was collected and incubated for 1 h at 4°C on a rotating shaker with 0.5-μg mouse IgG anti-PrP monoclonal antibody (SAF70, SAF37) or non-specific mouse control IgG. The immunocomplexes were then isolated using anti-mouse IgG Dynabeads (Invitrogen) according to the manufacturer's instructions and resuspended in 25-μl buffer A. Four microliters were kept for APE1gel cleavage assay and the remaining volume was boiled in Laemmli sample buffer and analyzed by SDS-PAGE electrophoresis and western blot as described.

Immunohistochemistry

After paraffin removal, tissue sections were boiled in a 10-mM citrate solution (pH6), washed in PBS and then incubated for 10 min in PBS, 1% SDS. After saturation for 30

min in PBS, 2% BSA, tissue sections were incubated for 45 min at 37°C with the monoclonal antibody Bar233 at 1:500 (Jacques Grassi, CEA Saclay) and washed in PBS, 2% BSA. Primary antibodies were revealed using IMPRESS anti-mouse Ig Polymer detection kit (Vector Laboratories) and counterstained with hematoxylin (Labonord). Pictures were recorded using a BX51 Olympus microscope coupled with a color video camera (Sony) and the Histolab software (Microvision Instruments, Evry, France).

Statistical analysis

Mann–Whitney statistical analysis was performed using the BioStaTGV online software.

RESULTS

In brain tissues, APE1 activity and DNA repair induction by a genotoxic stress are dependent on PrP induction

In order to explore the possibility of a link between PrP and DNA repair we compared the response of brain from wild-type and *Prnp*$^{-/-}$ mice to methyl-methanesulfonate (MMS), an alkylating agent that leads to high levels of AP sites in cellular DNA. MMS was chosen to avoid the pleiotropic effects and responses triggered by an oxidative stress. Animals were injected with MMS and the AP endonuclease activity was measured in brain homogenates 24 h after the treatment (Figure 1A). Interestingly, the basal levels of AP endonuclease activity were significantly lower in brain extracts from *Prnp*$^{-/-}$ animals than in those from the wild type. Moreover, while an induction of the activity was detected after MMS treatment of wild-type animals, this increase was completely absent in the *Prnp*$^{-/-}$ ones. Consistent with a compromised DNA repair capacity, the unrepaired AP sites remaining in the brain 24 h after the treatment were higher in the *Prnp*$^{-/-}$ brain cells than in those from wild-type animals (Figure 1B).

Figure 1C and Supplementary Figure S1B show that in spite of the higher Ape1 activity detected in the brains of wild-type animals, there was no correlation between the levels of Ape1 protein and the *Prnp* genotype, neither at the basal level nor after MMS injection. Surprisingly, evaluation of PrP protein levels in the same extracts showed a clear induction of PrP in response to the MMS injection (Figure 1C). The increase in PrP in response to the MMS injection was further confirmed by immunohistochemistry of the hippocampus (Figure 1D).

Taken together, these results indicate that PrP expression is induced in mouse brain in response to MMS and that this induction is required for an increase in AP endonuclease activity and a more efficient DNA damage repair in brain.

PrP levels determine neuronal cells DNA repair capacity and survival to genotoxic agents

We reasoned that if the PrP deficiency in mice resulted in an impaired DNA repair capacity, it should also sensitize brain cells to the genotoxic insult. To test this hypothesis we isolated neural stem and progenitor cells from either wild-type or *Prnp*$^{-/-}$ animals. Exposing these cells in primary culture to MMS triggered the induction of the PrP protein (Figure 1E). Moreover, *Prnp*$^{-/-}$ neuronal stem and progenitor cells displayed significantly higher levels of apoptotic cells than wild type (Figure 1F), indicating that PrP has a protective function against the DNA damaging agent.

To further define the relationship between the expression of PrP and the repair of abasic sites in mouse neurons, we compared the response to MMS of hippocampal HpL3–4 *Prnp*$^{-/-}$ cells expressing PrP (HpL-PrP) or not (HpL-EM) from a constitutive promoter. As observed in brain tissues, even though the levels of APE1 protein did not vary (Figure 2A), after exposure to the alkylating agent cells lacking PrP showed higher levels of induced AP sites than those expressing the protein (Figure 2B). Furthermore, HpL-EM cells displayed an impaired repair capacity compared to that of cells expressing PrP (Figure 2B). Consistent with this observation, APE1 activity was readily induced after MMS treatment in HpL-PrP but not in HpL-EM cells (Figure 2C). In order to confirm that the deficiency in repair detected in cells lacking PrP had consequences on their resistance to the alkylating agent, we monitored cell survival after exposure to MMS. We found that the PrP deficiency led to a sensitization of HPL-EM cells to the genotoxic agent (Figure 2D).

We then analyzed the correlation between PrP expression, AP site repair capacity and cell survival in the human neuroblastoma cell line SH-SY5Y. First, we attempted reducing the PrP cellular content by a siRNA approach. Treatment of the cells with the alkylating agent strongly induced the expression of PrP in cells transfected with the control siRNA (siRNA-Scr), whereas expression of the siRNA against *PRNP* (siRNA-PrP) blocked this induction (Figure 3A, upper panel). As observed in mouse brains, the increase in PrP levels in response to MMS was paralleled by the induction of the AP endonuclease activity, which was also blocked in cells expressing siRNA-PrP (Figure 3B). In spite of the increased activity in SH-SY5Y-siRNA-Scr cells exposed to MMS, no significant variations in the levels of the APE1 protein could be observed (Figure 3A, lower panel). In agreement with the blockage of the induction of APE1 activity, SHSY5Y-siRNA-PrP cells displayed a strong inhibition of AP sites repair (Figure 3C). The apparently slow repair observed as well as the continuing accumulation of damage suggests that significant amounts of MMS remain within the cell after the medium change. Moreover, the lack of PrP induction in SH-SY5Y-siRNA-PrP cells greatly impaired their survival following exposure to the alkylating agent (Figure 3D). To confirm the correlation between PrP levels and the DNA damage response (DDR), we took the complementary approach to the above experiments by stably overexpressing PrP in SH-SY5Y cells (Supplementary Figure S2A). Higher PrP levels did indeed result in an improved cell survival at high MMS concentration (Supplementary Figure S2B).

Because APE1 is the first common enzyme in the BER pathway, we reasoned that PrP could also regulate the cellular response to other kinds of genotoxic agents. In particular we were interested in analyzing a putative role of PrP in the regulation of APE1 activity in cells subjected to an oxidative stress. Confirming the protective effect of PrP in neurons exposed to oxidative conditions, we found

an enhanced sensitivity of SH-SY5Y-siRNA-PrP cells compared to those expressing the control siRNA after exposure to hydrogen peroxide (Figure 3E). Interestingly, exposure to H_2O_2 induced the APE1 activity in SH-SY5Y-siRNA-Scr cells, whereas inhibiting PrP expression in SH-SY5Y-siRNA-PrP cells abolished the induction of the AP endonuclease activity (Figure 3F). Oxidative treatment led to increased levels of PrP protein in the siRNA-Scr-transfected cells, whereas expression of APE1 remained unchanged (Figure 3G).

These results show that PrP is crucial in human and mouse neuronal cells to induce APE1 activity in response to genotoxic insult, including oxidative stress, thus allowing the repair of induced DNA lesions and cell survival.

Genotoxic stress leads to transcriptional activation of *PRNP*

The results obtained on brain (Figure 1C) and cell cultures (Figure 3A and G) showed an increase of PrP protein levels in response to DNA damaging agents. Since such an induction was not observed in the HpL-PrP cells where *PRNP* is expressed from a constitutive promoter (Figure 2A), we hypothesized that the endogenous *PRNP* promoter could be activated in response to the treatment. Quantitative RT-PCR analyses done on both SH-SY5Y-siScr and -siPrP cells at different times after exposure to either MMS (Figure 4A) or H_2O_2 (Figure 4B) showed a strong increase in *PRNP* transcripts in response to the genotoxic stresses, leading to a higher PrP cellular content (Figures 3G and 4C). For both genotoxic treatments, the induction of *PRNP* mRNA and protein levels was efficiently blocked by the siRNA against PrP (Figures 3G and 4C). Confirming that the increase in *PRNP* mRNA levels after MMS treatment is due to an activation of the *PRNP* promoter, we observed that actinomycin D completely blocked the induction in the *PRNP* mRNA levels in MMS-treated cells (Figure 4D).

PrP is found in the nucleus after genotoxic stress

Since in all cases presented above PrP induction in response to a genotoxic stress resulted in a stimulation of APE1 activity without a significant increase in APE1 protein levels (Figures 1C, 3A and G), we reasoned that PrP could interact functionally with APE1. However, while APE1 acts essentially in the nucleus, PrP is generally found as a membrane-associated protein, although its presence in the nucleus has been reported (30–33). We therefore decided to analyze by confocal microscopy the PrP subcellular localization in the brain from mice exposed to MMS. While no signal is detected in *Prnp*$^{-/-}$ (Figure 5A, upper panels), a specific labeling is observed in the hippocampus of wild-type-non-treated animals (Figure 5A, middle panels). However, 24 h after intra-peritoneal MMS injection, not only a clear increase in PrP levels but also an unambiguous nuclear localization of the protein was revealed in the same region of the brain (Figure 5A, lower panel).

To verify that PrP accumulated also in the nuclei of human SH-SY5Y neuroblastoma cells treated with a genotoxic agent, we analyzed the localization of the protein by immunofluorescence (IF) using two monoclonal antibodies against different PrP epitopes. As shown in Figure 5B,

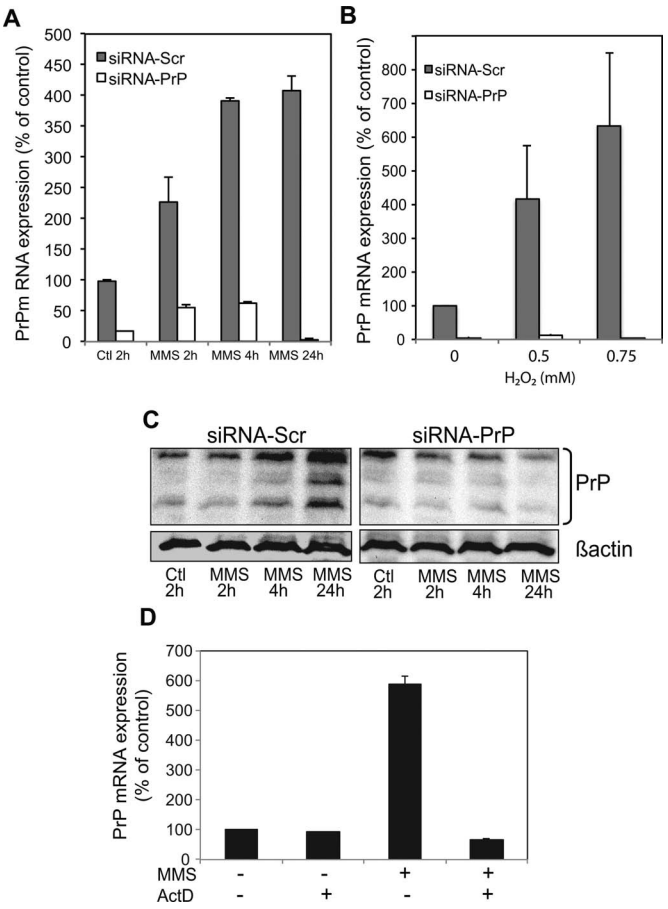

Figure 4. Genotoxic stress induces increased PrP protein levels through transcriptional activation of *PRNP*. (**A**) *PRNP* transcripts are induced after MMS treatment. RT-PCR analysis of *PRNP* mRNAs in SH-SY5Y cells transfected with siRNA PrP or with the scramble siRNA at different times following treatment with 1.5-mM MMS compared to untreated cells (Ctl) Mean ± SD ($n = 4$). (**B**) *PRNP* transcripts are induced after H_2O_2 treatment RT-PCR analysis of *PRNP* mRNAs in SH-SY5Y cells transfected with siRNA PrP or with the scramble siRNA at 24 h following treatment with 0.5- and 0.75-mM H_2O_2 compared to untreated cells (Ctl). Mean ± SD ($n = 4$). (**C**) PrP protein levels are induced after MMS treatment. Western blots for PrP at different times following 1-h exposure to 1.5-mM MMS of SH-SY5Y cells transfected with siRNA PrP or with the scramble siRNA. (**D**) Actinomycin D prevents the induction of *PRNP* mRNA in MMS-treated cells. RT-PCR analysis of PrP mRNAs in untreated SH-SY5Y cells or 4 h after exposure to 1.5-mM MMS in the presence or absence of actinomycin D.

PrP expression was highly increased after MMS exposure and, in addition to the classic membrane localization, we detected a strong signal for PrP in nuclei, where APE1 was also found. Because the presence of PrP in the nucleus was unexpected, we wondered whether the failure to detect a nuclear signal by IF in previous reports could, in part, be due to differences in the protocols used. Indeed, since detection of external membrane proteins does not require internalization of the antibodies for their recognition, most IF studies aiming at visualizing PrP do not include the permeabilization step. Figure 5C shows that the classic PrP localization pattern is indeed obtained in MMS-treated cells by omitting permeabilization. However, under those conditions even abundant nuclear proteins such as histone H4

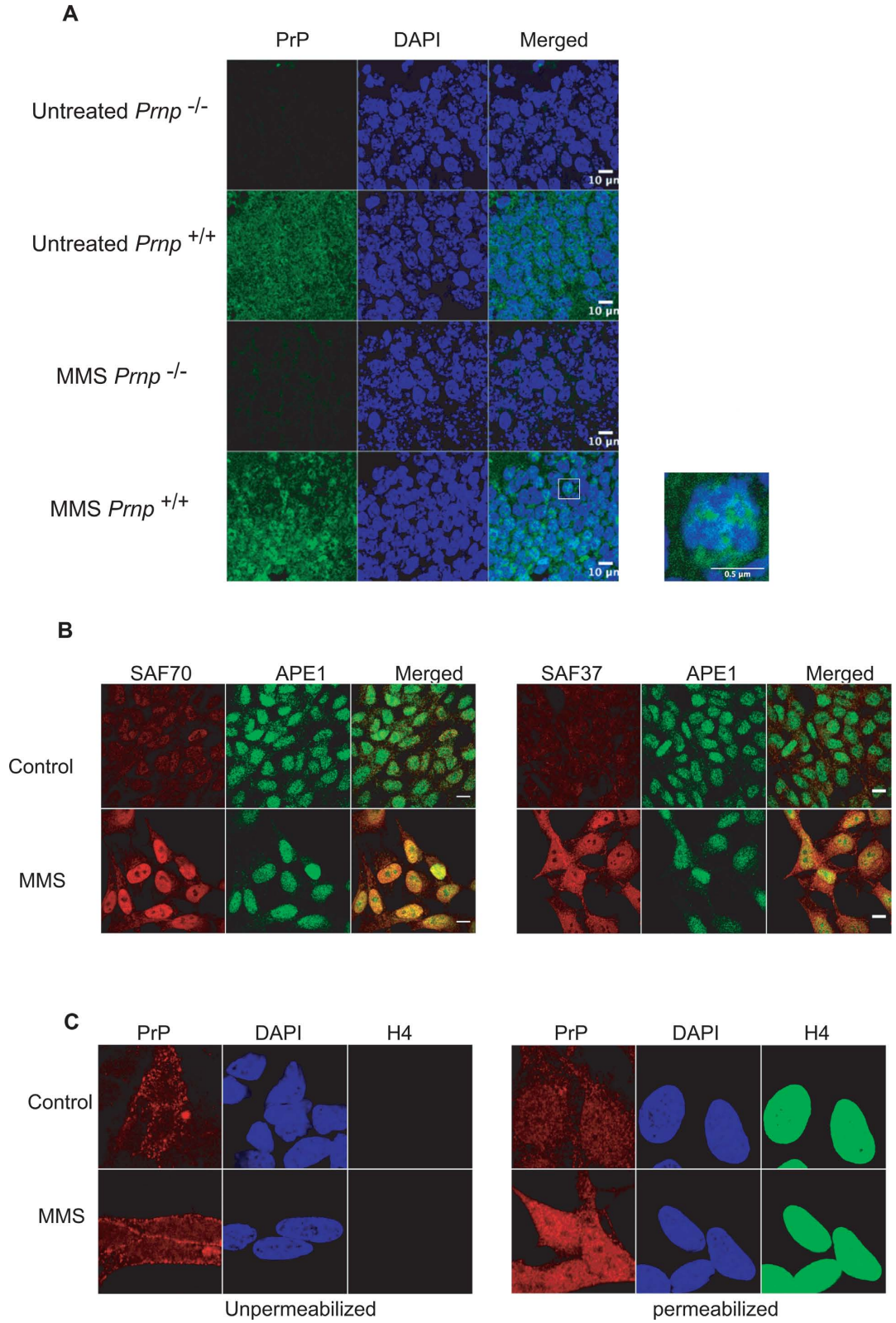

Figure 5. Genotoxic stress leads to accumulation of PrP in the nucleus of neuronal cells. (**A**) Increase of nuclear PrP in brain sections from *Prnp*$^{+/+}$ mice 24 h after MMS treatment (100 mg/kg) as detected by immunofluorescence. Brain sections from *Prnp*$^{-/-/-}$ animals were used as negative control. (**B**) Images obtained by confocal microscopy showing PrP and APE1 staining in SH-SY5Y cells 24 h after 1 h of treatment with 1.5-mM MMS as compared to untreated ones. Two different antibodies recognizing different epitopes of PrP were used: SAF70 (left panel) and SAF37 (right panel). (**C**) Detection of nuclear PrP requires permeabilization of the cells. PrP (SAF37 antibody) and histone H4 staining was performed on non-permeabilized (left panel) or permeabilized (right panel) control and MMS-treated SH-SY5Y cells.

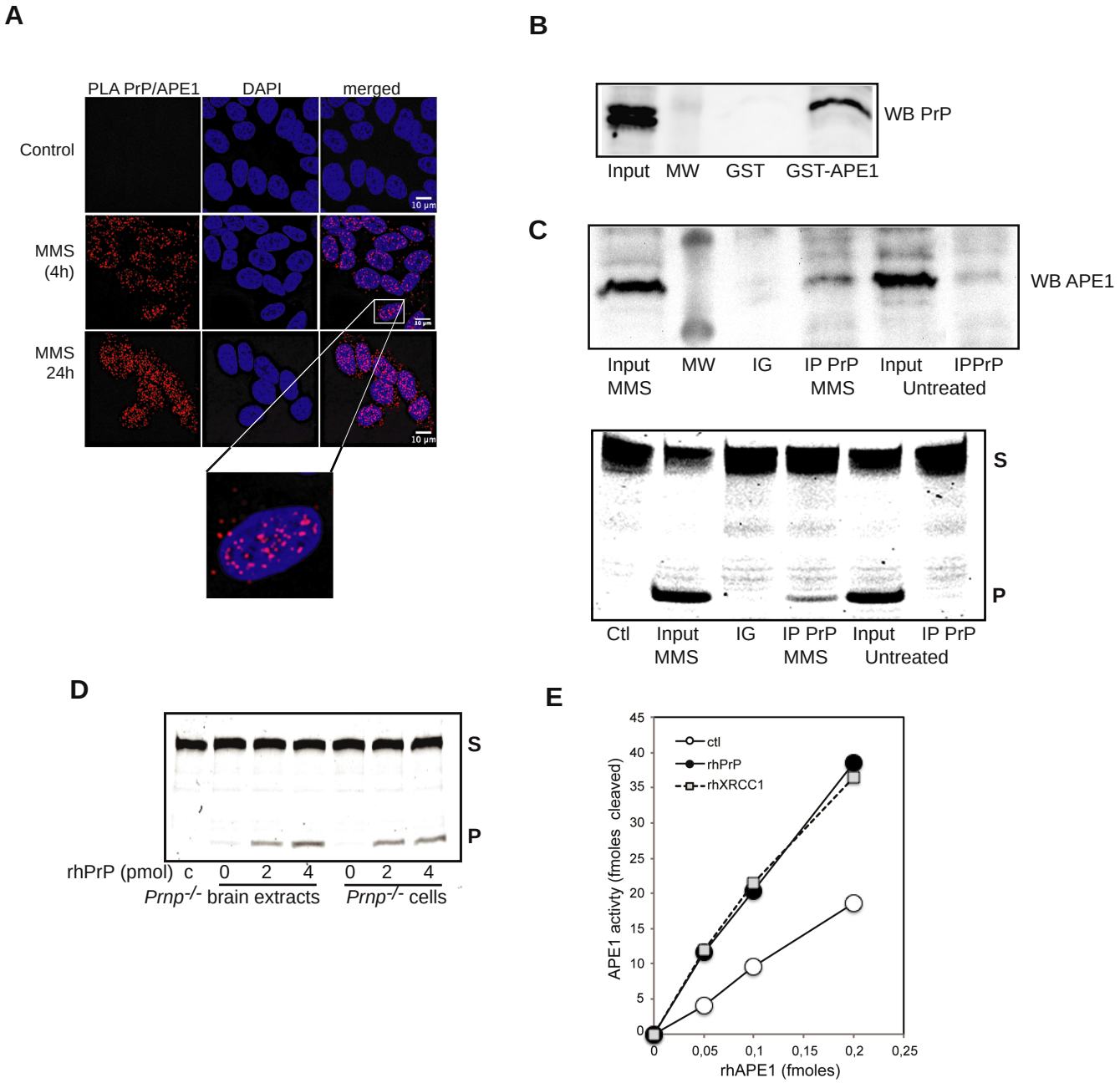

Figure 6. PrP interacts with APE1 and stimulates its endonuclease activity. (**A**) PLA assay shows the *in situ* close proximity of endogenous PrP and APE1 (red spots) mainly in cell nuclei (DAPI) at 4 and 24 h after MMS treatment of SH-SY5Y cells. (**B**) Protein extracts from SH-SY5Y cells treated with 1.5-mM MMS were subjected to GST-pull down assays using GST or GST-APE1. (**C**) Protein extracts from SH-SY5Y cells untreated or treated with 1.5-mM MMS were subjected to immunoprecipitation with antibodies against PrP and APE1 was detected by western blot (upper panel). Lanes IG and MW correspond to a non-specific antibodies and molecular weight markers, respectively. The presence of APE1 in the immunoprecipitate was also probed through an enzymatic activity assay by evaluating the conversion of the fluorescent tetrahydrofuran-containing oligonucleotide substrate (S) to the shorter incised product (P) (lower panel). (**D**) Representative gel showing the stimulation by human recombinant PrP (rhPrP) of the AP endonuclease activity of extracts from *Prnp*$^{-/-}$ brain and cells (20ng). Panel (C) corresponds to the oligonucleotide without any protein added. (**E**) Stimulation by rhPrP or rhXRCC1 (2 pmoles) of the endonuclease activity of purified human APE1.

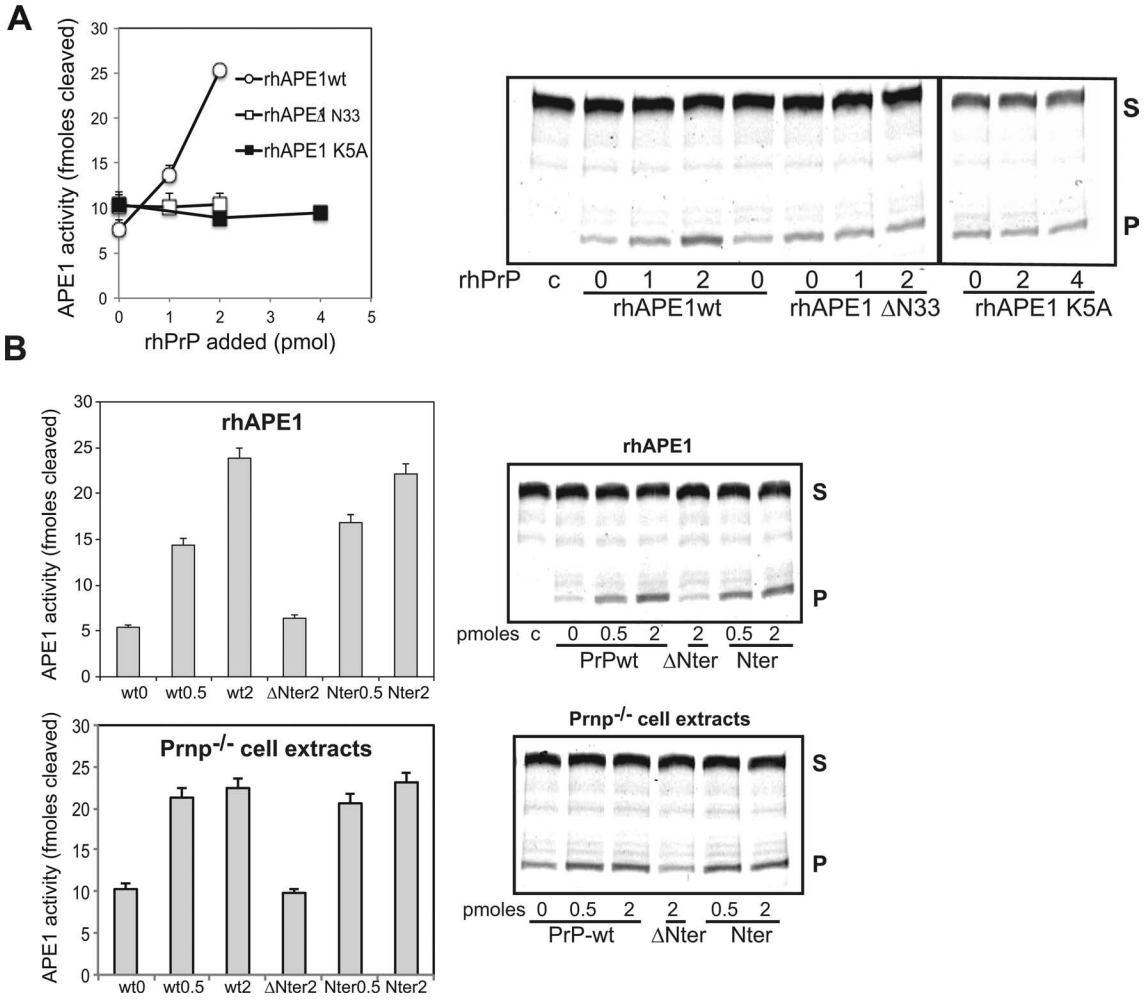

Figure 7. PrP-mediated stimulation of APE1 endonuclease activity involved the N-terminal part of each protein. (**A**) Stimulation by rhPrP of the endonuclease activity of the human wtAPE1, ΔN33APE1 and K5AAPE1. (**B**) Stimulation of the endonuclease activity of rhAPE1 (0.2 fmoles) or *Prnp*$^{-/-}$ cell extracts (20 ng) by the indicated amounts of ovine wtPrP, ΔNter (AA 103–232) and Nter (AA 23–124). For (A) and (B), data correspond to the average of three independent experiments. Representative activity gels are presented in each case (right panels).

are inaccessible to antibodies (Figure 5C, left panel). It is by adding the permeabilization step that nuclear proteins, such as the histone and the PrP nuclear fraction, can be detected (Figure 5C, right panel). Finally, to rule out that the nuclear signal observed was due to the internalization of the membrane-associated protein during the permeabilization procedure, SH-SY5Y cells exposed to MMS were treated with phosphoinositide phospholipase C (PIPLC) prior to PrP staining in order to eliminate the PrP present on the cell surface by cleavage of the protein from its GPI anchor. While in non-permeabilized cells treated with PIPLC essentially all the detectable PrP signal was lost, permeabilization allowed us to unambiguously detect the intracellular PrP fraction, in particular in the nucleus (Supplementary Figure S3A). The presence of PrP in the nucleus was further confirmed by subcellular fractionation of SH-SY5Y cells (Supplementary Figure S3B).

PrP interacts with APE1 and stimulates its DNA repair activity

We then addressed the possibility of a physical interaction between PrP and APE1. PLAs (29) showed that after MMS exposure PrP and APE1 are found within interaction distance from each other mainly in the nucleus (Figure 6A). Whereas a positive signal was found using XRCC1 and APE1, a known APE1 interactor (34), no signal of proximity was observed between PrP and XRCC1, confirming the specificity of the PLA assay using APE1 and PrP after genotoxic stress (Supplementary Figure S4). These results raised the possibility that stimulation of APE1 by PrP is the result of a direct interaction between the two proteins. GST pull-down experiments using a GST-APE1 fusion protein as bait confirmed this interaction in extracts from cells exposed to MMS (Figure 6B). The reciprocal experiment, immunoprecipitation of PrP, confirmed that active APE1 is specifically associated with the prion protein after genotoxic stress, as shown both by immunoblot against APE1 (Figure 6C, upper panel) and AP-endonuclease assays (Figure

6C, lower panel). To definitely assess the impact of PrP on APE1 activity, purified human recombinant PrP was added to AP endonuclease activity reactions with either *Prnp*$^{-/-}$ cell extracts or *Prnp*$^{-/-}$ brain homogenates. In both cases addition of recombinant PrP significantly increased AP endonuclease activity (Figure 6D). Control experiments with PrP alone demonstrated that the PrP protein itself has no AP-site incision activity (Supplementary Figure S5A). The stimulation of APE1 by PrP was further confirmed by measuring the activity of purified human APE1 in the presence of recombinant PrP. The stimulation of APE1 by PrP was comparable to that obtained with XRCC1, previously shown to be an inducer of APE1 endonuclease activity (34) (Figure 6E). Taken together these results confirm that PrP can directly stimulate the major AP endonuclease APE1.

Since stimulation of APE1 by several of its partners is mediated by the N-terminal domain of the protein through the presence of charged lysines (26), we asked whether these residues were also involved in the stimulation of APE1 activity by PrP. APE1 stimulation by PrP was abrogated by deletion of the first 33 amino acids of APE1 (ΔN-33) or mutation of its first five lysines into alanines (K5A) (Figure 7A). Similar results were obtained using recombinant ovine PrP (Supplementary Figure 5B). Based on the fact that the N-terminal part of PrP was shown to mediate its neuroprotective effect (35,36), we then checked if this region is also involved in the stimulatory effect on APE1 activity. We found that the N-terminal region is sufficient for stimulation of APE1 repair activity, whereas PrP deleted from its N-terminal part (ΔNter) is ineffective (Figure 7B).

DISCUSSION

PrP is a highly conserved protein predominantly expressed in neurons. Here, we have unveiled a major role for PrP in the maintenance of genomic stability after exposure to a genotoxic stress both in cultured neuronal cells and in mouse brain. Thus, our findings provide a new explanation for the previously described protective effect of PrP against oxidative conditions found both *in vitro* and *in vivo*. This novel function of PrP could be critical for limiting the long-term accumulation of DNA damage in neurons, consistent with the high level of basal expression of PrP in these specific cells that need to survive for decades.

We show here that an early event characterizing the protective effect of PrP is upregulation of *PRNP* gene expression. *PRNP* transcriptional activation was previously reported in neuronal cells exposed to oxidative stress conditions (37,38). Our results not only confirm these data but also show for the first time that *PRNP* gene expression is rapidly upregulated after exposure to MMS, suggesting that *PRNP* is involved in the DDR. This is consistent with the observed transcriptional activation of *PRNP* involving the ataxia telangiectasia-mutated (ATM) pathway after a copper-induced oxidative stress (38). Interestingly, ATM signaling is known to be triggered by MMS-induced DNA damage (39) and to activate BER (40) after exposure of cells to the alkylating agent. These observations together with the results presented here further support the involvement of PrP in the DDR.

We show here that PrP interacts with and stimulates APE1, a central component of the BER system required for the protection of neurons against oxidative stress (19–21). In this way the induction of PrP boosts cell DNA repair capacity and favors survival to genotoxic stresses. Although PrP is mainly considered a membrane-anchored protein, there are evidences pointing to its presence in the nucleus (30,31,33,41,42), thus potentially allowing an interaction with APE1. The identification of several proteins with affinity for nucleic acids as PrP interactors also suggested a nuclear function for PrP (43). Notably, PrP interacts with the N-methylpurine DNA glycosylase whose role is to remove alkylated bases, just upstream of APE1 in the BER of MMS-induced DNA lesions. The idea of a role for PrP in DNA repair is further supported by its affinity for nucleic acids (44) and its capacity to bend and unwind DNA (45,46). Moreover, it was recently demonstrated that it interacts with chromatin histones (33,47). Our results raise the question of how PrP, a protein normally going through the glycosylation pathway, can, in response to a genotoxic stress, be directed to the cell nucleus. Although the underlying mechanisms are still unclear, several groups have also found that glycosylated forms of PrP are localized to the cell nucleus (33,41,42). Consistently, cryptic nuclear localization signal sequences in the C-terminal part of PrP have been identified (48). Alternative mechanisms involving retrograde intracellular transport (49–52) or internalization (53) can also be invoked and should be explored. Thus, the ability of PrP to be directed to the nucleus and modulate DNA or chromatin structures is in agreement with a role in the recruitment and activation of DNA repair proteins inferred from our results.

We find here that the stimulation of APE1 activity by PrP is mediated by the flexible N-terminal part of the protein. Interestingly, the positively charged N-terminal domain of PrP is required for its DNA binding activity (45,46) as well as for its protective activity against stress (35). Moreover, expression of a N-terminal truncated PrP in mice leads to ataxia and cerebellar lesions, a phenotype that could be rescued by the introduction of a single copy of the wild-type gene (4). More recently, it was reported that the N-terminal domain of the protein is critical for its neuroprotective activity in mice (54), underscoring the importance of this domain in PrP function.

Stimulation of APE1 endonuclease activity by PrP requires the presence of five charged lysines within the first 33 amino acids of the N-terminal region of APE1, the same region required for the stimulation by XRCC1 (34) and NPM1 (26,28). These critical residues were shown to regulate APE1 catalytic activity on abasic DNA by stabilizing, through electrostatic binding, the enzyme on the reaction product (26).

Several observations suggest that the reduced APE1 activity in *Ape1* heterozygous mice and the impairment of its induction in *Prnp*$^{-/-}$ mice share some common consequences. Indeed, the 2-fold reduction in Ape1 activity due to haploinsufficiency was found to be sufficient to alter DNA repair efficiency and to increase cell death in mice subjected to a genotoxic stress (18). Similarly, PrP-deficiency and Ape1 haploinsufficiency each renders cells more sensitive to apoptosis (55,56). Interestingly, as it is the case for

Prnp$^{-/-}$ mice, *Ape1* heterozygous mice, in spite of their reduced repair capacity, do not show any overt phenotype in normal conditions nor do they display a predisposition to cancer (16,18). The reduced APE1 activity in *Ape1*$^{+/-}$ mice only favors cancer development in response to genotoxic stress when combined with deficiencies in other DNA repair or apoptosis pathways (57,58). Interestingly, a recent report showed that animals genetically impaired for BER of oxidative DNA damage show an accelerated progression of prion-induced symptoms (59). This, together with the results presented here, raises the intriguing possibility that aggregation of PrP during disease might lead to the loss of the normal PrP role in activating DNA repair, accelerating therefore neuronal cell death.

In conclusion, this study reveals a new physiological function of PrP as a strong activator of DNA damage repair through stimulation of the central base excision repair enzyme, the AP endonuclease APE1. PrP would thus be required to maintain genetic stability in cells subjected to either endogenous or exogenous stresses leading to increased levels of ROS and thus to elevated generation of AP sites. This function might be impaired in any pathology characterized by PrP modifications and increased oxidative stress, leading to accumulation of mutations or to cell death. Considering the ubiquitous expression of the PrP-encoding gene in mammalian tissues, this DNA protection pathway is likely to operate in cell types other than neurons.

SUPPLEMENTARY DATA

Supplementary Data are available at NAR Online.

ACKNOWLEDGEMENTS

We thank Human Rezaei and Vincent Béringue (INRA, Jouy-en Josas) for mouse PrP vector and recombinant PrP proteins; Jacques Grassi (CEA Saclay) for the antibodies against PrP; Charles Weissmann (Institute of Neuropathology, University Hospital Zurich) for the *Prnp*$^{-/-}$ mice; Franck Mouthon and Paul Brown (CEA Fontenay-aux-roses) for comments and discussions; Audrey Rouaix for her help with animal experiments; and Thierry Kortulewski for his help with the IF analyses carried out at the IRCM microscopy facility.

FUNDING

Commissariat à l'Energie Atomique (CEA) Radiobiology Programme [to A.B.]; INSERM [to UMR967]; Postdoctoral Fellowships from the Région Ile de France (DIM-Sent 2009 program) and the Eurotalents Program [to D.F.]; MIUR [FIRB_RBRN07BMCT, PRIN2008_CCPKRP_003 to G.T.]; AIRC [IG10269 to G.T.]. Funding for open access charge: Commissariat à l'Energie Atomique.
Conflict of interest statement. None declared.

REFERENCES

1. Westergard,L., Christensen,H.M. and Harris,D.A. (2007) The cellular prion protein (PrP(C)): its physiological function and role in disease. *Biochim. Biophys. Acta*, **1772**, 629–644.
2. Linden,R., Martins,V.R., Prado,M.A., Cammarota,M., Izquierdo,I. and Brentani,R.R. (2008) Physiology of the prion protein. *Physiol. Rev.*, **88**, 673–728.
3. Biasini,E., Turnbaugh,J.A., Unterberger,U. and Harris,D.A. (2012) Prion protein at the crossroads of physiology and disease. *Trends Neurosci.*, **35**, 92–103.
4. Shmerling,D., Hegyi,I., Fischer,M., Blattler,T., Brandner,S., Gotz,J., Rulicke,T., Flechsig,E., Cozzio,A., von Mering,C. *et al.* (1998) Expression of amino-terminally truncated PrP in the mouse leading to ataxia and specific cerebellar lesions. *Cell*, **93**, 203–214.
5. Solomon,I.H., Schepker,J.A. and Harris,D.A. (2010) Prion neurotoxicity: insights from prion protein mutants. *Curr. Issues Mol. Biol.*, **12**, 51–61.
6. Brown,D.R., Nicholas,R.S. and Canevari,L. (2002) Lack of prion protein expression results in a neuronal phenotype sensitive to stress. *J. Neurosci. Res.*, **67**, 211–224.
7. Vassallo,N. and Herms,J. (2003) Cellular prion protein function in copper homeostasis and redox signalling at the synapse. *J. Neurochem.*, **86**, 538–544.
8. Choi,C.J., Anantharam,V., Saetveit,N.J., Houk,R.S., Kanthasamy,A. and Kanthasamy,A.G. (2007) Normal cellular prion protein protects against manganese-induced oxidative stress and apoptotic cell death. *Toxicol. Sci.*, **98**, 495–509.
9. McLennan,N.F., Brennan,P.M., McNeill,A., Davies,I., Fotheringham,A., Rennison,K.A., Ritchie,D., Brannan,F., Head,M.W., Ironside,J.W. *et al.* (2004) Prion protein accumulation and neuroprotection in hypoxic brain damage. *Am. J. Pathol.*, **165**, 227–235.
10. Spudich,A., Frigg,R., Kilic,E., Kilic,U., Oesch,B., Raeber,A., Bassetti,C.L. and Hermann,D.M. (2005) Aggravation of ischemic brain injury by prion protein deficiency: role of ERK-1/-2 and STAT-1. *Neurobiol. Dis.*, **20**, 442–449.
11. Nicolas,O., Gavin,R. and Rio,J.A. (2009) New insights into cellular prion protein (PrPc) functions: the 'ying and yang' of a relevant protein. *Brain Res. Rev.*, **61**, 170–184.
12. Senator,A., Rachidi,W., Lehmann,S., Favier,A. and Benboubetra,M. (2004) Prion protein protects against DNA damage induced by paraquat in cultured cells. *Free Radic. Biol. Med.*, **37**, 1224–1230.
13. Watt,N.T., Routledge,M.N., Wild,C.P. and Hooper,N.M. (2007) Cellular prion protein protects against reactive-oxygen-species-induced DNA damage. *Free Radic. Biol. Med.*, **43**, 959–967.
14. Lindahl,T. (1993) Instability and decay of the primary structure of DNA [see comments]. *Nature*, **362**, 709–715.
15. Xanthoudakis,S., Smeyne,R.J., Wallace,J.D. and Curran,T. (1996) The redox/DNA repair protein, Ref-1, is essential for early embryonic development in mice. *Proc. Natl. Acad. Sci. U.S.A.*, **93**, 8919–8923.
16. Meira,L.B., Devaraj,S., Kisby,G.E., Burns,D.K., Daniel,R.L., Hammer,R.E., Grundy,S., Jialal,I. and Friedberg,E.C. (2001) Heterozygosity for the mouse Apex gene results in phenotypes associated with oxidative stress. *Cancer Res.*, **61**, 5552–5557.
17. Fung,H. and Demple,B. (2005) A vital role for Ape1/Ref1 protein in repairing spontaneous DNA damage in human cells. *Mol. Cell*, **17**, 463–470.
18. Unnikrishnan,A., Raffoul,J.J., Patel,H.V., Prychitko,T.M., Anyangwe,N., Meira,L.B., Friedberg,E.C., Cabelof,D.C. and Heydari,A.R. (2009) Oxidative stress alters base excision repair pathway and increases apoptotic response in apurinic/apyrimidinic endonuclease 1/redox factor-1 haploinsufficient mice. *Free Radic. Biol. Med.*, **46**, 1488–1499.
19. Vasko,M.R., Guo,C. and Kelley,M.R. (2005) The multifunctional DNA repair/redox enzyme Ape1/Ref-1 promotes survival of neurons after oxidative stress. *DNA Repair*, **4**, 367–379.
20. Huang,E., Qu,D., Zhang,Y., Venderova,K., Haque,M.E., Rousseaux,M.W., Slack,R.S., Woulfe,J.M. and Park,D.S. (2010) The role of Cdk5-mediated apurinic/apyrimidinic endonuclease 1 phosphorylation in neuronal death. *Nat. Cell Biol.*, **12**, 563–571.
21. Stetler,R.A., Gao,Y., Zukin,R.S., Vosler,P.S., Zhang,L., Zhang,F., Cao,G., Bennett,M.V. and Chen,J. (2010) Apurinic/apyrimidinic endonuclease APE1 is required for PACAP-induced neuroprotection against global cerebral ischemia. *Proc. Natl. Acad. Sci. U.S.A.*, **107**, 3204–3209.

22. Bueler,H., Aguzzi,A., Sailer,A., Greiner,R.A., Autenried,P., Aguet,M. and Weissmann,C. (1993) Mice devoid of PrP are resistant to scrapie. *Cell*, **73**, 1339–1347.
23. Fischer,M., Rulicke,T., Raeber,A., Sailer,A., Moser,M., Oesch,B., Brandner,S., Aguzzi,A. and Weissmann,C. (1996) Prion protein (PrP) with amino-proximal deletions restoring susceptibility of PrP knockout mice to scrapie. *EMBO J.*, **15**, 1255–1264.
24. Pineda,J.R., Daynac,M., Chicheportiche,A., Cebrian-Silla,A., Sii Felice,K., Garcia-Verdugo,J.M., Boussin,F.D. and Mouthon,M.A. (2013) Vascular-derived TGF-beta increases in the stem cell niche and perturbs neurogenesis during aging and following irradiation in the adult mouse brain. *EMBO Mol. Med.*, **5**, 548–562.
25. Rezaei,H., Marc,D., Choiset,Y., Takahashi,M., Hui Bon Hoa,G., Haertle,T., Grosclaude,J. and Debey,P. (2000) High yield purification and physico-chemical properties of full-length recombinant allelic variants of sheep prion protein linked to scrapie susceptibility. *Eur. J. Biochem.*, **267**, 2833–2839.
26. Fantini,D., Vascotto,C., Marasco,D., D'Ambrosio,C., Romanello,M., Vitagliano,L., Pedone,C., Poletto,M., Cesaratto,L., Quadrifoglio,F. *et al.* (2010) Critical lysine residues within the overlooked N-terminal domain of human APE1 regulate its biological functions. *Nucleic Acids Res.*, **38**, 8239–8256.
27. Marsin,S., Vidal,A.E., Sossou,M., Menissier-de Murcia,J., Le Page,F., Boiteux,S., de Murcia,G. and Radicella,J.P. (2003) Role of XRCC1 in the coordination and stimulation of oxidative DNA damage repair initiated by the DNA glycosylase hOGG1. *J. Biol. Chem.*, **278**, 44068–44074.
28. Vascotto,C., Fantini,D., Romanello,M., Cesaratto,L., Deganuto,M., Leonardi,A., Radicella,J.P., Kelley,M.R., D'Ambrosio,C., Scaloni,A. *et al.* (2009) APE1/Ref-1 interacts with NPM1 within nucleoli and plays a role in the rRNA quality control process. *Mol. Cell. Biol.*, **29**, 1834–1854.
29. Soderberg,O., Leuchowius,K.J., Gullberg,M., Jarvius,M., Weibrecht,I., Larsson,L.G. and Landegren,U. (2008) Characterizing proteins and their interactions in cells and tissues using the in situ proximity ligation assay. *Methods*, **45**, 227–232.
30. Hosokawa,T., Tsuchiya,K., Sato,I., Takeyama,N., Ueda,S., Tagawa,Y., Kimura,K.M., Nakamura,I., Wu,G., Sakudo,A. *et al.* (2008) A monoclonal antibody (1D12) defines novel distribution patterns of prion protein (PrP) as granules in nucleus. *Biochem. Biophys. Res. Commun.*, **366**, 657–663.
31. Morel,E., Fouquet,S., Strup-Perrot,C., Pichol Thievend,C., Petit,C., Loew,D., Faussat,A.M., Yvernault,L., Pincon-Raymond,M., Chambaz,J. *et al.* (2008) The cellular prion protein PrP(c) is involved in the proliferation of epithelial cells and in the distribution of junction-associated proteins. *PLoS One*, **3**, e3000.
32. Rybner,C., Finel-Szermanski,S., Felin,M., Sahraoui,T., Rousseau,C., Fournier,J.G., Seve,A.P. and Botti,J. (2002) The cellular prion protein: a new partner of the lectin CBP70 in the nucleus of NB4 human promyelocytic leukemia cells. *J. Cell. Biochem.*, **84**, 408–419.
33. Strom,A., Wang,G.S., Picketts,D.J., Reimer,R., Stuke,A.W. and Scott,F.W. (2011) Cellular prion protein localizes to the nucleus of endocrine and neuronal cells and interacts with structural chromatin components. *Eur. J. Cell Biol.*, **90**, 414–419.
34. Vidal,A.E., Boiteux,S., Hickson,I.D. and Radicella,J.P. (2001) XRCC1 coordinates the initial and late stages of DNA abasic site repair through protein-protein interactions. *EMBO J.*, **20**, 6530–6539.
35. Sakthivelu,V., Seidel,R.P., Winklhofer,K.F. and Tatzelt,J. (2011) Conserved stress-protective activity between prion protein and Shadoo. *J. Biol. Chem.*, **286**, 8901–8908.
36. Beland,M. and Roucou,X. (2012) The prion protein unstructured N-terminal region is a broad-spectrum molecular sensor with diverse and contrasting potential functions. *J. Neurochem.*, **120**, 853–868.
37. Shyu,W.C., Lin,S.Z., Saeki,K., Kubosaki,A., Matsumoto,Y., Onodera,T., Chiang,M.F., Thajeb,P. and Li,H. (2004) Hyperbaric oxygen enhances the expression of prion protein and heat shock protein 70 in a mouse neuroblastoma cell line. *Cell. Mol. Neurobiol.*, **24**, 257–268.
38. Qin,K., Zhao,L., Ash,R.D., McDonough,W.F. and Zhao,R.Y. (2009) ATM-mediated transcriptional elevation of prion in response to copper-induced oxidative stress. *J. Biol. Chem.*, **284**, 4582–4593.
39. Barfknecht,T.R. and Little,J.B. (1982) Hypersensitivity of ataxia telangiectasia skin fibroblasts to DNA alkylating agents. *Mutat. Res.*, **94**, 369–382.
40. Chou,W.C., Wang,H.C., Wong,F.H., Ding,S.L., Wu,P.E., Shieh,S.Y. and Shen,C.Y. (2008) Chk2-dependent phosphorylation of XRCC1 in the DNA damage response promotes base excision repair. *EMBO J.*, **27**, 3140–3150.
41. Crozet,C., Vezilier,J., Delfieu,V., Nishimura,T., Onodera,T., Casanova,D., Lehmann,S. and Beranger,F. (2006) The truncated 23–230 form of the prion protein localizes to the nuclei of inducible cell lines independently of its nuclear localization signals and is not cytotoxic. *Mol. Cell. Neurosci.*, **32**, 315–323.
42. Juanes,M.E., Elvira,G., Garcia-Grande,A., Calero,M. and Gasset,M. (2009) Biosynthesis of prion protein nucleocytoplasmic isoforms by alternative initiation of translation. *J. Biol. Chem.*, **284**, 2787–2794.
43. Satoh,J., Obayashi,S., Misawa,T., Sumiyoshi,K., Oosumi,K. and Tabunoki,H. (2009) Protein microarray analysis identifies human cellular prion protein interactors. *Neuropathol. Appl. Neurobiol.*, **35**, 16–35.
44. Lima,L.M., Cordeiro,Y., Tinoco,L.W., Marques,A.F., Oliveira,C.L., Sampath,S., Kodali,R., Choi,G., Foguel,D., Torriani,I. *et al.* (2006) Structural insights into the interaction between prion protein and nucleic acid. *Biochemistry*, **45**, 9180–9187.
45. Bera,A., Roche,A.C. and Nandi,P.K. (2007) Bending and unwinding of nucleic acid by prion protein. *Biochemistry*, **46**, 1320–1328.
46. Guichard,C., Ivanyi-Nagy,R., Sharma,K.K., Gabus,C., Marc,D., Mely,Y. and Darlix,J.L. (2011) Analysis of nucleic acid chaperoning by the prion protein and its inhibition by oligonucleotides. *Nucleic Acids Res.*, **39**, 8544–8558.
47. Cai,H., Xie,Y., Hu,L., Fan,J. and Li,R. (2013) Prion protein (PrP) interacts with histone H3 confirmed by affinity chromatography. *J. Chromatogr. B Analyt. Technol. Biomed. Life Sci.*, **929C**, 40–44.
48. Gu,Y., Hinnerwisch,J., Fredricks,R., Kalepu,S., Mishra,R.S. and Singh,N. (2003) Identification of cryptic nuclear localization signals in the prion protein. *Neurobiol. Dis.*, **12**, 133–149.
49. Beranger,F., Mange,A., Goud,B. and Lehmann,S. (2002) Stimulation of PrP(C) retrograde transport toward the endoplasmic reticulum increases accumulation of PrP(Sc) in prion-infected cells. *J. Biol. Chem.*, **277**, 38972–38977.
50. Hachiya,N.S., Watanabe,K., Yamada,M., Sakasegawa,Y. and Kaneko,K. (2004) Anterograde and retrograde intracellular trafficking of fluorescent cellular prion protein. *Biochem. Biophys. Res. Commun.*, **315**, 802–807.
51. Ma,J. and Lindquist,S. (2001) Wild-type PrP and a mutant associated with prion disease are subject to retrograde transport and proteasome degradation. *Proc. Natl. Acad. Sci. U.S.A.*, **98**, 14955–14960.
52. Restelli,E., Fioriti,L., Mantovani,S., Airaghi,S., Forloni,G. and Chiesa,R. (2010) Cell type-specific neuroprotective activity of untranslocated prion protein. *PLoS One*, **5**, e13725.
53. Kang,Y.S., Zhao,X., Lovaas,J., Eisenberg,E. and Greene,L.E. (2009) Clathrin-independent internalization of normal cellular prion protein in neuroblastoma cells is associated with the Arf6 pathway. *J. Cell Sci.*, **122**, 4062–4069.
54. Turnbaugh,J.A., Westergard,L., Unterberger,U., Biasini,E. and Harris,D.A. (2011) The N-terminal, polybasic region is critical for prion protein neuroprotective activity. *PLoS One*, **6**, e25675.
55. Huamani,J., McMahan,C.A., Herbert,D.C., Reddick,R., McCarrey,J.R., MacInnes,M.I., Chen,D.J. and Walter,C.A. (2004) Spontaneous mutagenesis is enhanced in Apex heterozygous mice. *Mol. Cell. Biol.*, **24**, 8145–8153.
56. Kuwahara,C., Takeuchi,A.M., Nishimura,T., Haraguchi,K., Kubosaki,A., Matsumoto,Y., Saeki,K., Matsumoto,Y., Yokoyama,T., Itohara,S. *et al.* (1999) Prions prevent neuronal cell-line death. *Nature* **400**, 225–226.
57. Cheo,D.L., Meira,L.B., Burns,D.K., Reis,A.M., Issac,T. and Friedberg,E.C. (2000) Ultraviolet B radiation-induced skin cancer in mice defective in the Xpc, Trp53, and Apex (HAP1) genes: genotype-specific effects on cancer predisposition and pathology of tumors. *Cancer Res.* **60**, 1580–1584.
58. Meira,L.B., Cheo,D.L., Hammer,R.E., Burns,D.K., Reis,A. and Friedberg,E.C. (1997) Genetic interaction between HAP1/REF-1 and p53. *Nat. Genet.* **17**, 145.
59. Jalland,C.M., Benestad,S.L., Ersdal,C., Scheffler,K., Suganthan,R., Nakabeppu,Y., Eide,L., Bjoras,M. and Tranulis,M.A. (2014) Accelerated clinical course of prion disease in mice compromised in repair of oxidative DNA damage. *Free Radic. Biol. Med.* **68**, 1–7.